Implementation of decoherence-protected logical qubits in medium-size Josephson-junction arrays.

B. Douçot* and L. B. Ioffe†

*Laboratoire de Physique Théorique et Hautes Énergies, CNRS UMR 7589, Universités Paris 6 et 7, 4, place Jussieu, 75252 Paris Cedex 05 France

†Center for Materials Theory, Department of Physics and Astronomy, Rutgers University 136 Frelinghuysen Rd., Piscataway NJ 08854 USA

Abstract. We outline the physical principles underlying the design of finite size superconducting arrays that may serve as protected qubits. These systems are built from fully frustrated rhombi consisting of four Josephson junctions; their low energy spectrum is composed of localized Z_2 charge excitations and π phase vortices. Protection from both the phase and flip errors requires a balance between charging and Josephson energies; optimization of the array size results in the hierarchical construction of these arrays. We have developed computational methods, based on a combination of perturbation theory and numerical diagonalization, which allow us to compute the global phase stiffness and the energy of localized charge excitations in various geometries. We present the most promising designs, which are currently under experimental investigation.

Keywords: Topological protection, Josephson junction arrays, qubits
PACS: 03.67.Lx,74.81.Fa

INTRODUCTION

The goal of this paper is to identify and to compute the properties of the small to medium sized Josephson junction arrays which spectrum contains two low energy states that are protected from the external noise and can be used as protected qubits for quantum computation. Such arrays provide a minimalistic implementation of the idea of topologically protected quantum computation that was introduced by Kitaev in his seminal paper [1] and developed for large and medium sized Josephson junction arrays in [2],[3], [4]. The mathematical models describing the low energy dynamics of these arrays can be also regarded as the Hamiltonian implementation of quantum error correction algorithms. [5]

The elementary building block of all arrays considered here is the four junction superconducting loop threaded by the magnetic flux $\Phi = \Phi_0/2$ that we shall call rhombus in the following, see Fig. 1. The effective Josephson energy $V(\theta)$ of the *ideal* rhombus is a π- periodic function of the phase difference across it; most of our discussion below is applicable to any element that has *approximately* this property. In the case of rhombus, $V(\theta)$ has two minima at $\theta = \pm\pi/2$, separated by π modulo 2π. In the absence of transitions between these states induced by quantum fluctuations the ground state of each element is doubly degenerate. The π- periodicity for $V(\theta)$ can be interpreted in simple physical terms by noting that Fourier decomposition of $V(\theta) = \sum_n A_n e^{in\theta}$ contains only even harmonics, that is $A_n = 0$ for all odd values of n. The absence of all odd harmonics and, in particular, the suppression of the fundamental oscillation ($n = \pm 1$) means that single Cooper pairs cannot tunnel across the individual element and thus are localized. For the element realized as a rhombus threaded by half a flux quantum, the localization occurs due to the cancellation between the probability amplitudes for a Cooper pair to follow the upper and the lower arms of the rhombus while tunneling across. A single rhombus is *not* protected against local noise: flux deviations from the $\Phi_0/2$, scatter of junction parameters lead to non-zero tunneling amplitude of a single pair (odd harmonics $A_n \neq 0$) which lifts the degeneracy of the two states. Fluctuations of this amplitude lead to the fast dephasing of such elementary qubit.

This description of a single π- periodic element and its dephasing suggests that a stronger protection against flux noise may be achieved by composing N such elements in a series which makes the single pair tunneling exponentially small. Indeed, the global state of the system is described by the phase difference ϕ between the ends of the chain which is equal to the sum $\phi = \sum_{j=1}^{N} \theta_j$ of the phase differences, θ_j across individual elements. The energy of the system is also a π- periodic function of ϕ for the chain composed of ideal elements. Let us first assume that the quantum fluctuations of ϕ are small, which can be achieved in practice by introducing a large capacitance between the two ends of the chain. In this case, the system has two global states corresponding to two minima of the total energy as a function of the phase ϕ. Because the absolute value of the phase is not measurable these two states become ideally protected from the

decoherence in the limit $N \to \infty$ provided that the energy barrier separating them remains finite. For a finite L this protection is only as good as a suppression of a single pair tunneling along the whole chain. This suppression is possible thanks to a remarkable property of arrays composed of π- periodic elements: in these arrays the parity of the number of Cooper pairs on each node joining two or more elements becomes a good quantum number in the absence of external noise or any static imperfection. As will be explained later, these local conserved quantities can be viewed as the eigenvalues of local Z_2 symmetries generators that translate the phase at a given node by π while leaving phases on other nodes unchanged.

The protection provided by a single chain depends crucially on the ratio E_C/E_J of the charging energy E_C to Josephson energy E_J. In the limit when the charging energy E_C is much smaller than the Josephson energy E_J, the quantum fluctuations of phase variables are small and therefore, the energy difference between the even and odd parity states on a given node is small as well. In this limit the noise and imperfections have large effect on these almost degenerate states and can transfer the Cooper pair across. The increase in E_C/E_J increases quantum phase fluctuations, and yields a finite energy gap Δ between the states with different parities. In the presence of flux noise of typical magnitude $\delta\Phi$ per rhombus, a single Cooper pair tunneling amplitude across each rhombus of order $\frac{\delta\Phi}{\Phi_0}E_J$ is generated. The dangerous process that transfers a single Cooper pair across the whole system arises only at order N in perturbation theory, therefore its amplitude is proportional to $(\frac{\delta\Phi}{\Phi_0}E_J)^N/\Delta^{N-1}$, which can be made arbitrarily small by choosing N large enough as long as $\frac{\delta\Phi}{\Phi_0}\frac{E_J}{\Delta} < 1$. This basic protection mechanism has been recently demonstrated experimentally by the observation of a strong reduction of the single Cooper pair tunneling amplitude for a flux per rhombus Φ close to $\Phi_0/2$ in a system with $N = 4$, compared to one with $N = 2$. [6]

So far, we discussed how to achieve protection against processes that lift the degeneracy between the two classical ground states identified by the value of the phase variable ϕ. We now turn to the tunneling processes between the classical ground states which are made possible by the finite capacitance across the chain. Their effect is to lift the degeneracy in the ground-state doublet and to select the basis in which the operator giving parity of the number of Cooper pairs transferred across the whole chain is diagonal. The amplitude of this process is sensitive to the electrostatic potential across the whole chain which might fluctuate. This would lead to the fluctuations of the energy splitting and thus dephasing. As we already pointed out, the tunneling might be inhibited by large capacitance between the ends of the chain. However, such capacitance would also imply that corresponding charging energy is small which would make it difficult to avoid thermal activation in the realistic setup. It would be very desirable to reduce the tunneling between classical ground states exponentially fast in the system size, as for the single Cooper pair tunneling along the whole chain discussed above. Note that a process that translates ϕ by π may be viewed as a single π vortex crossing the chain. A natural way to suppress such events is to couple M identical Z_2 chains in parallel. As we shall see, there is to some extent a conflict between the two requirements of imposing simultaneously a good localization of single Cooper pairs through a large gap Δ for a Z_2 charge in the bulk of the array, and a large energy barrier, $2E_2$ for a π vortex crossing: the former requires rather large quantum phase fluctuations (thus large E_C/E_J) and large chain length N whereas the latter needs a large phase stiffness so that E_C/E_J and the chain length cannot be too large. To resolve this conflict we shall use the hierarchical construction which uses iteratively series and parallel compositions of arrays whose building blocks are rhombi threaded by half a flux quantum.

Note that whereas it is possible to suppress completely single Cooper pair tunneling in ideal conditions in a single chain by having exactly half a flux quantum and a perfect mirror symmetry along the diagonal for each rhombus, reduction of the π vortex tunneling amplitude is only achieved by choosing a low enough value of E_C/E_J and remains non-zero for any non-zero value of this parameter. In other words, for these arrays there is no analogue of the local Z_2 symmetry that would prevent single π vortex tunneling; these arrays do not implement exactly the self dual model proposed by Kitaev [1] Nevertheless, as we shall demonstrate, the proper choice of the array geometry that involves parallel chains of rhombi and a proper choice of the E_C/E_J ratio allow for the exponentially high protection against any local noise for large arrays and a very strong (power law) noise suppression for medium size ones.

The medium sized arrays most promising for implementation are characterized by large gap Δ and large π vortex barrier, $2E_2$. Because both are the functions of E_C/E_J we compare different designs by values of the gap Δ at E_C/E_J that correspond to the crossing of these two curves, i.e. $\Delta = E_2$. Becuase the medium sized arrays are too large for direct numerical diagonalization in the relevant parameter regimes, in order to compute this important parameter we shall have to develop the approximate analytical and numerical methods for this problem.

The protection provided by the system of parallel chains of π- periodic elements can be understood as the Hamiltonian version of the error correction based on the repetition code. In this code one uses $N \times M$ faulty qubits to encode one logical qubit. At the first stage of this construction one forms 2 classical states $|C0>$ in each of the N qubits: $|C0>=|00...0>$ and $|C1>=|11...1>$. This

classical repetition protects against X errors that change 0 into 1 or backwards. At the second stage one forms quantum superposition of these two states $|\pm>=(|C0>\pm|C1>)$ in each of these M rows and takes the direct product of the resulting states:

$$|\pm\rangle = \begin{pmatrix} \frac{1}{\sqrt{2}}(|0000\rangle_1 \pm |1111\rangle_1)\otimes \\ \frac{1}{\sqrt{2}}(|0000\rangle_2 \pm |1111\rangle_2)\otimes \\ \frac{1}{\sqrt{2}}(|0000\rangle_3 \pm |1111\rangle_3)\otimes \\ \frac{1}{\sqrt{2}}(|0000\rangle_4 \pm |1111\rangle_4) \end{pmatrix} \qquad (1)$$

This step protects against Z-errors that change the relative phase of individual $|0>$ and $|1>$ states and, thus, flip $|\pm>$ states.

In order to establish the correspondence between the array of Josephson junctions and the array of qubits we identify the rhombus states $|\pm\pi/2\rangle$ with the states of spin $1/2$ with $S_z = \pm 1/2$, the low energy states of the rhombi array are equivalent to the states of the spin array of the same size. The actual Josephson circuit has also high energy modes with $E_p \sim \sqrt{8E_J E_C}$, which are separated from the low energy states by a large gap and thus can be mostly ignored. Identifying $|0\rangle$ ($|1\rangle$) of the faulty qubit with the even (odd) states of individual rhombus ($|e\rangle = (|+\pi/2\rangle + |-\pi/2\rangle)/\sqrt{2}$, $|o\rangle = (|+\pi/2\rangle - |-\pi/2\rangle)/\sqrt{2}$), we see that $(|0000\rangle_1 \pm |1111\rangle_1)/2$ state of a qubit chain corresponds to state rhombi chain in which all rhombi are in even or odd states with the phase difference across the chain $\pm\pi/2$ respectively.

The idea of the physical array construction is therefore to ensure that its ground state corresponds to the 'ferromagnetic' state of one chain in the charge (odd/even) basis and to the equal phase difference across different the chains. The former is ensured by the Hamiltonian $H = \sum_{(i,i')} \sigma_i^x \sigma_{i'}^x$ where the sum is over all pairs (i,i') belonging to the same chain. The low energy states of each chain correspond to the codewords in which all spins point in the same direction along x-axis, i.e. to $\prod_i |e\rangle_i$ and $\prod_i |o\rangle_i$ states in each chain. The parallel connection of the chains ensures that all signs ($+$ or $-$) in (1) are the same, thereby protecting against $Z-$errors.

Similarly to a repetition code that can determine up to $(N-1)$ Z-errors and $(M-1)$ X-errors in the system of M chains of length N, the Hamiltonian version that we discuss in this paper is protected to the order of N against the dephasing and to the order of M against the decay. The main difference between the physical systems that we discuss here and the mathematical error correction models is due to the existence of other low energy modes that are ignored in their mapping to the chain of $1/2$ spins.

Although this is not directly relevant for engineering protected qubits, we briefly mention here that these arrays characterized by the two types of elementary excitations (Z_2 charges and π vortices) are quite interesting systems from the viewpoint of statistical physics, because the unbroken local Z_2 symmetry leads to the destruction of the usual Cooper pair condensate: on any island j connecting two rhombi in the bulk, the values ϕ_j and $\phi_j + \pi$ for the local phase are equiprobable and therefore the superconducting order parameter $\langle e^{i\phi_j}\rangle$ vanishes. On the other hand, $\langle e^{i2\phi_j}\rangle$ should be non-zero in order to prevent the proliferation of π vortices. These arrays therefore realize condensates of pairs of Cooper pairs without the condensation of single Cooper pairs, a regime that may be qualified as superconducting nematic. [2, 7, 8]

MODEL AND ITS LOCAL Z_2 SYMMETRY

Model

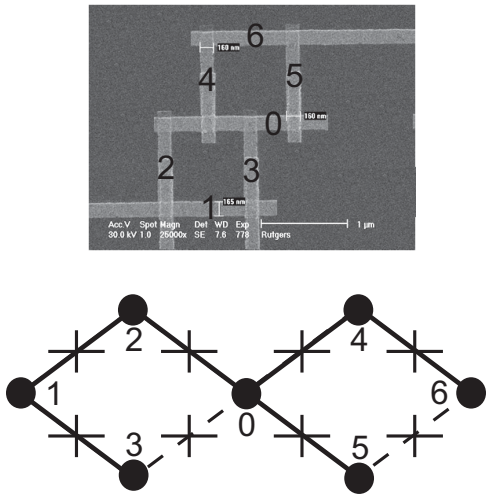

FIGURE 1. Schematics of the simplest protected array (lower pane) and the microphotogaph of its implementation in the Al nano-structure (upper pane). The basic element of all protected arrays the rhombus formed by four junctions (crosses) and four islands (dots), e.g. islands $0,1,2,3$ or $0,4,5,6$ which is frustrated by magnetic flux equal to one half of the flux quantum. In the implementation the islands are horizontal or vertical lines, the junctions are formed at each intersection. The line style in the schematics represents the choice of vector potentials used to encode the magnetic flux: thick lines denote zero vector potential while dashed lines denote vector potential that shifts by π the relation between current and phase difference accross such junctions. As explained in the text, the unique properties of the arrays are due to the local Z_2 transformations, such as the one centered around site 0 that flips the chiralities of these two rhombi without changing the phases at the two outer sites labelled by 1 and 6.

We shall consider Josephson junction arrays described by the standard Hamiltonian:

$$H = 4E_{\rm C}\sum_{ij}\hat{n}_i(\mathscr{C}^{-1})_{ij}\hat{n}_j - E_{\rm J}\sum_{\langle ij\rangle}\mathscr{J}_{ij}\cos(\phi_i-\phi_j) \quad (2)$$

where $\mathscr{C}_{ij}$ is the dimensionless capacitance matrix measured in units of the capacitance C of individual junctions, and the charging energy $E_{\rm C}$ is defined by $E_{\rm C} = e^2/(2C)$ (corresponding to single electron charging energy). The dimensionless matrix $\mathscr{J}_{ij}$ encodes the Josephson couplings: $\mathscr{J}_{ij} = \pm 1$ when i and j refer to nearest neighbor sites, and $\mathscr{J}_{ij} = 0$ otherwise. The signs in the $\mathscr{J}_{ij}$ variables are required in order to implement the fully frustrated array with one half of a flux quantum per elementary plaquette. In this case, the product of $\mathscr{J}_{ij}$'s over each such plaquette has to be equal to -1. $E_{\rm J}$ is the Josephson coupling energy of individual junctions. The number operators $\hat{q}_j$ are conjugate to the local phases ϕ_j, namely: $\hat{q}_j = \frac{1}{i}\frac{\partial}{\partial\phi_j}$. It will be also convenient to write down the corresponding Lagrangian, because it involves the capacitance matrix that is a much more local object than its inverse:

$$L = \sum_{\langle ij\rangle}\frac{1}{16E_{\rm C}}(\dot{\phi}_i-\dot{\phi}_j)^2 + E_{\rm J}\sum_{\langle ij\rangle}\mathscr{J}_{ij}\cos(\phi_i-\phi_j) \quad (3)$$

To simplify the notation, we have assumed $\hbar = 1$ in the expression of the kinetic term.

For the computation of large arrays and for the qualitative discussion of their properties it is convenient to model each fully frustrated rhombus by an effective junction that transfers coherently pairs of Cooper pairs. The Josephson energy of such an element (that will be called a Z_2 junction) may be written as $-E_2\cos 2(\phi_i-\phi_j)$ and its charging energy is incorporated in the Lagrangian by the same term $\frac{1}{16E_{\rm C}^{\rm eff}}(\dot{\phi}_i-\dot{\phi}_j)^2$ as before. Note that in the classical limit, $E_{\rm C}^{\rm eff} = E_{\rm C}$ because a rhombus involves two chains of two elementary junctions in parallel.

Local Z_2 symmetry

As we have emphasized in the Introduction, we shall construct protected qubits from networks of superconducting islands connected by fully frustrated rhombi. In such systems single Cooper pairs are localized in Aharonov-Bohm cages centered at each node of the network and the parity of the number of Cooper pairs contained in each cage is conserved. [8] These conserved quantities can be viewed as the generators of local discrete Z_2 symmetries which we now define. Let us for instance consider the geometry of Fig. 1 with a pair of two adjacent rhombi that share the node labelled by 0.

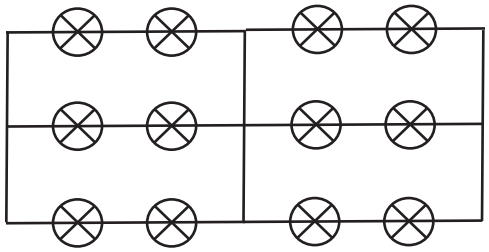

FIGURE 2. The array with twelve elementary rhombi (shown as crossed circles), organized in three chains of four rhombi coupled by a central island in the middle.

The local Z_2 transformation centered on this node flips simultaneously the chiralities of the two rhombi adjacent to it while keeping fixed the phases of the outer sites 1 and 6. More precisely, it corresponds to the simultaneous changes:

$$\begin{aligned}
\phi_0 &\rightarrow \phi_0+\pi\\
\phi_2 &\rightarrow \phi_3\\
\phi_3 &\rightarrow \phi_2\\
\phi_1 &\rightarrow \phi_1\\
\phi_4 &\rightarrow \phi_5+\pi\\
\phi_5 &\rightarrow \phi_4+\pi\\
\phi_6 &\rightarrow \phi_6
\end{aligned}$$

Clearly, such transformation leaves invariant the Josephson energy associated to this circuit, that is:

$$\begin{aligned}
H_{\rm J} &= -\cos(\phi_1-\phi_2)-\cos(\phi_2-\phi_0)-\cos(\phi_1-\phi_3)\\
&+ \cos(\phi_3-\phi_0)-\cos(\phi_0-\phi_4)-\cos(\phi_4-\phi_6)\\
&- \cos(\phi_0-\phi_5)+\cos(\phi_5-\phi_6)
\end{aligned}$$

It also preserves the kinetic terms in the Lagrangian, because the above transformation simply permutes the time derivatives of phase variables according to the mirror symmetry along the axis joining the central site 0 with the two extremal points 1 and 6. Note that experimentally, this requires a rather high reproducibility of the junction parameters across the array, because we need a perfect symmetry between the upper and lower sides of any rhombus.

It is also convenient to express the same symmetry operation in the charge basis. It sends a wave function ψ of q_0,...,q_6 into the new wave function ψ' defined by:

$$\begin{aligned}
&\psi'(q_0,q_1,q_2,q_3,q_4,q_5,q_6) =\\
&\quad e^{i\pi(q_0+q_4+q_5)}\psi(q_0,q_1,q_3,q_2,q_5,q_4,q_6) \quad (4)
\end{aligned}$$

The presence of the phase factor $e^{i\pi q_0}$ suggests that this unitary operation is directly related to the parity of the number of Cooper pairs on the node 0. However, this

operation is slightly more complicated, because it also involves the mirror symmetry along the horizontal diagonals of the two rhombi and additional π translations of phases at sites 4 and 5. A more precise connection can be obtained in the framework of a Bose Hubbard model. There, the Josephson coupling is represented by a single boson hopping process. It is therefore possible to diagonalize this Hamiltonian (in the presence of the magnetic field of half flux quantum per rhombus); this yields Wannier orbitals localized in finite clusters of sites centered on the nodes that share two or more rhombi. In this version, the local Z_2 generator centered at a given node counts precisely the parity of the number of bosons in the localized orbitals centered on this node. [8] In this paper, we shall not use the Bose Hubbard model, but rather the quantum rotor Hamiltonian version Eq. (2).

In this work we shall mostly consider coupled chains of rhombi and some generalizations such as the one depicted on Fig. 2. For this array we have six binary flips associated to the middle islands of the six two rhombi subchains, and one six-fold flip of all the six rhombi adjacent to the central island. It is easy to generalize the precise definition of the local Z_2 flips given above to the case of a node connected to an arbitrary number of rhombi. One can then check that two local Z_2 transformations centered on different nodes mutually commute.

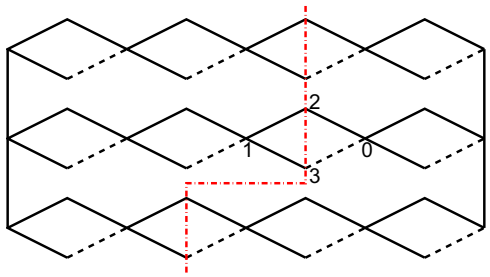

FIGURE 3. (Color online) An example of a non local Z_2 unitary transformation in an array with three coupled chains of four rhombi. The red dashed dotted line indicates the set of rhombi which chirality flips under the transformation. Phases on all islands located on the left (resp. right) of this line are unchanged (resp. shifted by π). For sites located precisely on the line, they exchange their phase with the site opposite to them on the same rhombus. For example, phases at sites 2 and 3 are permuted.

As we discuss below, the low energy spectra of large arrays can be reproduced in a coarse grained picture in which the array is built from *effective* Z_2 junctions, i.e. elements doubly periodic in the phase variable. In this picture the local symmetries take a simpler form, because the Z_2 generator based at node j shifts ϕ_j by π while leaving all the other phases unchanged. In this situation, it is exactly the operator that counts the parity of the number of Cooper pairs on this node.

For the discussion of protected qubits, it is also important to mention the existence of non local Z_2 symmetries in which the local chirality variables are flipped for a subset of rhombi located on a line that cuts the array in two parts. An example is shown on Fig. 3. For a rhombus on this line, such as the one with sites labelled 0,1,2 and 3 on the figure, the transformation rules are as before, namely:

$$\begin{aligned} \phi_0 &\rightarrow \phi_0+\pi \\ \phi_2 &\rightarrow \phi_3 \\ \phi_3 &\rightarrow \phi_2 \\ \phi_1 &\rightarrow \phi_1 \end{aligned}$$

Phases on sites located on the left of the line are unchanged whereas those on sites located on the right are shifted by π. As a result the total phase difference π between the right and the left boundaries is also shifted by π. As mentioned in the Introduction, the physical meaning of such symmetry is the absence of any process that transfers an odd number number of Cooper pairs from one boundary to the other.

HIERARCHICAL CONSTRUCTION

Motivation

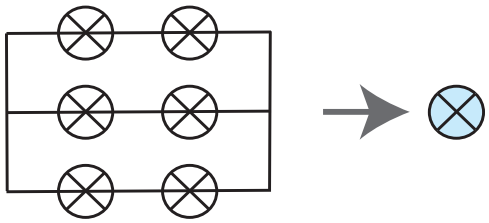

FIGURE 4. Hierarchical construction: the element at level $n+1$ is obtained by connecting in parallel K identical chains made of two elements at level n

As discussed in the Introduction, a large number of parallel chains of rhombi provides a good protection from the environment provided that quantum fluctuations of rhombi in each chain are strong but the phase difference between the ends of the chains does not fluctuate due to a large number of chains. The last requirement is not easy to satisfy for moderately long chains because the phase stiffness decreases exponentially with the length. [9] The alternative solution is to couple chains in the transverse direction. If this coupling is achieved by rhombi as well, one ends up with the full blown decorated lattice. Although possible, this design has a disadvantage that quantum fluctuations need to be strong enough to result in a simultaneous flip of many rhombi that have a common site and requires a large number of rhombi, all this is not easy to achieve practically.

The attractive alternative that we explore here is to use the hierarchical construction that does not involve additional elements in transverse direction. This construction has two substeps at each level. First, two Josephson elements formed at nth level are connected in series forming a weaker Josephson element. Second, K such Josephson elements are connected in parallel compensating this weakening and forming an effective element of the (n+1)th level. The idea is to choose the parameters so that the effective Josephson energy $E_2\cos(2\theta)$ and charging energy keep constant ratio at each level. This implies that quantum fluctuations remain strong but do not wash out the phase stiffness in a large structure. Provided that the $E_1\cos(\theta)$ term was significantly smaller than $E_2\cos(2\theta)$ at the first stage of the hierarchy, it will decrease exponentially with the level.

Hierarchical construction

The recursion relation that relates the energy scales at the next hierarchy level to the ones at the previous level can be obtained analytically in the limit of large branching ratio, K. In this limit, E_2/E_C for the individual junction is small which allows to treat them perturbatively.

A general (super) junction can be characterized by three parameters:

$$H = -E_2\cos 2\theta - E_1\cos\theta + 4E_C q^2$$

where q is the charge conjugate to the phase measured in units of $2e$. Two such junctions connected in series give a Josephson energy:

$$H = -E_2'\cos 2\theta - E_1'\cos\theta + 4E_C' q^2$$

Generally, one expects that the parameters of this element are some functions of the energies characterizing the original junctions:

$$E_2' = g_2(\frac{E_2}{E_C},\frac{E_1}{E_C})E_C \quad (5)$$

$$E_1' = g_1(\frac{E_2}{E_C},\frac{E_1}{E_C})E_C \quad (6)$$

$$E_C' = h(\frac{E_2}{E_C},\frac{E_1}{E_C})E_C \quad (7)$$

In the following we shall be mostly interested in the limit of very small $\frac{E_1}{E_C} \ll 1$. In this limit g_2 becomes a function of only one variable, $\frac{E_2}{E_C}$. Perturbative expansion gives:

$$E_2' = \frac{1}{8}\frac{E_2^2}{E_C} \quad (8)$$

$$E_1' = \frac{1}{2}\frac{E_1^2}{E_C} \quad (9)$$

$$E_C' = 2E_C \quad (10)$$

for sufficiently large E_C (perturbation theory in E_2/E_C). In this limit of small E_2/E_C the charging energy of the two elements connected in series is twice E_C.

Combining K such chains in parallel we get that at the next stage of the hierarchy:

$$E_C^{(n+1)} = (2/K)E_C^{(n)} \quad (11)$$

$$\frac{E_2^{(n+1)}}{E_C^{(n+1)}} = \frac{K^2}{16}\left[\frac{E_2^{(n)}}{E_C^{(n)}}\right]^2 \quad (12)$$

One can treat the block formed by $2K$ Josephson elements as a single junction characterized by only one degree of freedom provided that the energy scales at the next step are much smaller than the ones at the previous step. This is satisfied if $K \gg 1$ because in this limit the typical energy scales are set by $E_C^{(n)}$ that decreases with the level n. Thus, in this limit, the equations (11-12) become exact and show the (unstable) fixed point:

$$\frac{E_2^{(n)}}{E_C^{(n)}} = \frac{16}{K^2} \quad (13)$$

At realistic values of the branching number $K = 2-4$ one expects two types of corrections to this simple recursion. First, the perturbation expansion that gives (8) and $E_C' = 2E_C$ is not exact. Second, characteristic energy scales at the next level are not much smaller than the ones at the previous level and that makes coarse graining only approximate. We now discuss the importance of these corrections in turn. Calculation of the next order in perturbation theory gives:

$$E_C' = \left[1 - \frac{1}{16}\left(\frac{E_2}{E_C}\right)^2\right]2E_C \quad (14)$$

$$E_2' = \left[1 - \frac{7}{256}\left(\frac{E_2}{E_C}\right)^2\right]\frac{1}{8}\frac{E_2^2}{E_C} \quad (15)$$

that shows that the corrections to the perturbative result become significant for $E_2 \gtrsim 2E_C$. Thus, the equation for the fixed point (13) remains approximately valid down to $K = 3$. At small branching numbers the time scales do not grow fast with the level and this introduces an additional source of corrections. To check the accuracy of the recursion relations and the perturbative approximation we performed a numerical study comparing the effective Josephson energy E_2 expected from the recursion relations at the second level of hierarchy with the numerical diagonalization of the Hamiltonian that describes the system shown in Fig. 6a. We check separately the accuracy of the perturbative expansion by comparing the results (8), (15) with the diagonalization of two contacts connected in series, and the accuracy of the recursion by

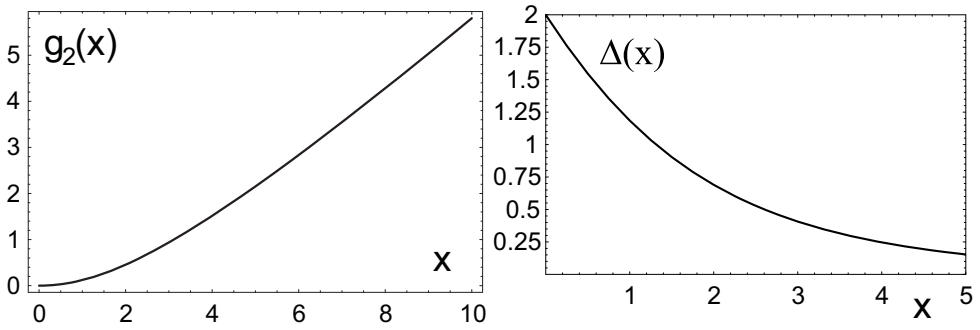

FIGURE 5. (a) Amplitude of the second harmonics $g_2(x)$ of the Josephson energy versus phase difference across two identical $E_2\cos(2\theta)$ junctions connected in series where $x = E_2/E_C$. (b) The energy of the lowest excited state corresponding to one Cooper pair at the middle island.

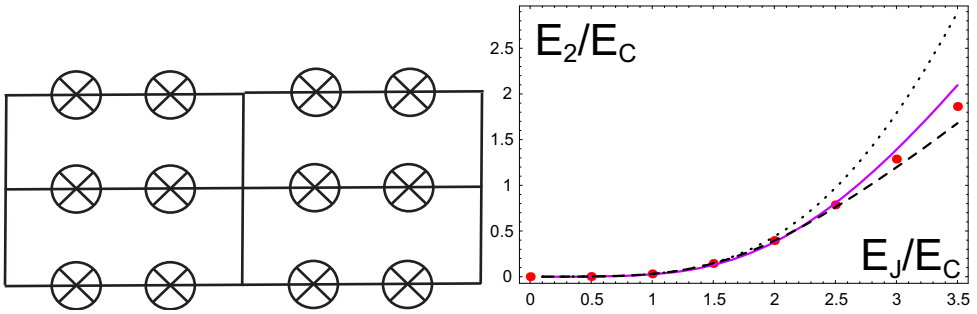

FIGURE 6. (a) The stage intermediate between levels 1 and 2 of the hierarchy with $K = 3$ branching made from the $\cos 2\theta$ elementary blocks used for testing the validity of the recursive approximation. (b) Exact diagonalization results for the effective E_2 (in the units of bare charging energy) of this element is shown as dots. The curves correspond to different approximate schemes. The full line is the result of the recursive approximation discussed in the text applied twice. The dotted line is the result of the diagonalization of the series of four junctions with additional capacitance $K-1$ in the middle and an overal multipying factor of K^2, according to the the form suggested by the perturbation theory in E_2/E_C.

comparing the effective Josephson energy E_2 found numerically with

$$E_2 = g_2\left(\frac{K^2 g_2(E_2/E_C)}{h(E_2/E_C)}\right)\frac{1}{K}h(E_2/E_C)E_C \qquad (16)$$

where $g_2(E_2/E_C)$ was evaluated numerically (see Fig. 5a) and we used the perturbative result $h(x) \approx 2 - 1/8x^2$. The result of the comparison is shown in Fig. 6b, where one observes that the recursive approximation (16) reproduces the exact results with a good accuracy even for $K = 3$ in the physically important range of the parameters $0 < E_2/E_C < 3$. We note that the results deviate lightly at low values, the reason can be understood by comparing the results obtained in the recursion approximation with the direct perturbation theory for the second level device.

The lowest order of the perturbation theory correspond to a sequence of charge tunnelings and charge-hole creations each of which moves charge in the same direction. The constraint that the process should occur with the minimal number of steps implies that a given sequence involves only one (out of K) branches of the device at each side. The remaining $K-1$ branches provide the additional capacitance attached to the middle island. Thus, in this order, the circuit can be replaced by a series of four basic elements, with the central island capacitively coupled to the ground, provided that the final result is multiplied by K^2. In the limit of large $K \gg 1$ the energy of the charge at the middle island is low in $1/K$.

The condition that process occurs in the minimal number of steps does preclude intermediate states that contain more than one charge or hole. However, in the limit of large K the dominant contribution comes only from the processes that involve the intermediate state in which the only charge is located at the middle island because this state has parametrically smaller charging energy $(16/K)E_C$. Keeping only these terms reproduces exactly the recursion result in which g_2 and h functions are approximated by their lowest order expressions (8), (10):

$$E_2^{pert} \approx \frac{K^3}{2^{10}}\left(\frac{E_2}{E_C}\right)^4 E_C \qquad (17)$$

At finite values of K, three effects combine to modify this result. First, the expression for g_2 at the first step

has to be modified to take into account the effect of the larger structure on the energy of virtual charged excitations between two elementary blocks. Specifically, the prefactor $1/8$ now becomes $1/(8+4/K)$. Second, some processes do not involve intermediate states with the charge located only on the middle island. Summing these effects, we get:

$$E_2^{pert} = \frac{K^4(K+2)}{2^8(2K+1)^2}\left(\frac{E_2}{E_C}\right)^4 E_C \qquad (18)$$

Third, the energy of the intermediate state with one charge on the middle island differs from $(16/K)E_C$ due to capacitance renormalization by virtual processes, but this occurs at higher order in E_2/E_C. For physically relevant $K=3$ the exact perturbation result (18) differs from the recursive approximation (17) by 20%.

Medium size rhombi arrays

For experimental implementations of protected qubits with superconducting circuits, the simplest way to get a π periodic element is to use a rhombus frustrated by half a flux quantum. In this sub-section, we shall discuss computational issues raised by the treatment of networks of rhombi. From the perspective of numerical diagonalizations, these networks involve very large Hilbert spaces, even for small sizes and moderate values of E_J/E_C. For example, a chain of four rhombi has 12 degrees of freedom which implies diagonalization in $10^{10}-10^{12}$ dimensional space for $E_J/E_C \lesssim 8$. Therefore, it is essential to develop approximate but reliable computation schemes for the low energy spectrum that allow for a significant reduction in the size of the Hilbert space. A natural coarse-graining procedure is to try to replace each rhombus by an effective Z_2 junction. As we have seen in section , this operation preserves the existence of a local Z_2 symmetry which implies that only pairs of Cooper pairs can propagate coherently across the network.

Generally, the dynamics of Z_2 junction is fully characterized its action $S(\theta)$ which is a non-local function of the phase θ across it. For the slow phase dynamics the action is separated into kinetic and potential part, for former can be approximated by quadratic form

$$\frac{1}{16E_C^{eff}}\int dt\,\dot{\theta}^2$$

where $E_C^{\rm eff}$ is its effective charging energy. The potential energy part can be characterized by the coefficients E_n in the expansion of the Josephson energy $V(\theta)=\sum E_n \cos n\theta$. Numerical diagonalization of the single rhombus shows that all E_n with $n>2$ are very small in the relevant parameter range $E_J/E_C \lesssim 8$ and can be safely neglected. So, in this approximation the effective Z_2 junction representing the rhombus is characterized by three parameters: E_1, E_2 and $E_C^{\rm eff}$. The accuracy of this approximation will be discussed below. The effective E_1 for an ideal rhombus vanishes exactly at all orders in E_J/E_C. The effective E_2 is generated starting from the fourth order in E_J/E_C. At this order, we have:

$$E_2 = \frac{7}{64}\frac{E_J^4}{E_C^3} \qquad (19)$$

The exact result for E_2 as a function of E_J/E_C is shown on Fig. 7.

We now turn to the effective charging energy. At very small E_J the tunneling of the charge can be neglected and the effective charging energy is given by electrostatics: $E_C^{\rm eff}=E_C$. However, we expect rather large corrections to this result in the relevant range of $2 \lesssim E_J/E_C \lesssim 8$ due to the charge delocalization which should lead to a decrease in the value of $E_C^{\rm eff}$. Estimating the effective capacitance first raises the issue of defining it precisely. In Eq. (14), this quantity has been computed for a series of two Z_2 junctions, to second order in E_J/E_C. This computation has been performed by first assuming a slow variation (on the scale $\hbar/E_C$) of the phase ϕ across the two junction chain, and then integrating out the internal phase degree of freedom. It is only in this limit, and to the lowest order in perturbation theory, that the effective action keeps the local $\dot{\phi}^2$ form that allows the straightforward definition of a renormalized capacitance. In general, we expect the effective action to become non-local in time, and even non-linear in $\dot{\phi}$. Furthermore, such a path integral approach is not as directly numerically implementable as a Hamiltonian formulation. Therefore, we shall adopt here the following procedure. We consider a series of two identical rhombi, with an additional capacitance C_0 on its rightmost island. This capacitance is introduced in order to slow down the quantum dynamics of the phase ϕ on this island, it also mimics the effect of the remaining part of the array. Then the gap between the ground-state and the first excited state with an odd charge on the intermediate island is computed by numerical diagonalization, for various values of E_J/E_c and C_0. This gap is also computed for a series of two Z_2 junctions, for which E_2 is chosen to be the one previously computed on Fig. 7 and where $E_C^{\rm eff}$ is adjusted in order to match the gaps for the odd intermediate charge sector of both systems. The values of $C_{\rm eff}$ ($E_C^{\rm eff}=2e^2/C_{\rm eff}$) as a function of E_J/E_C for $C_0=2,6$, and 10 are shown on Fig. 7. These curves show clearly a tendency for $C_{\rm eff}$ to saturate to a value around $3.5C$ as soon as $E_J/E_C \gtrsim 4$, and provided that $C_0 \gtrsim 5E_C$. This stability of $C_{\rm eff}$ is expected from physical considerations, because a large C_0 turns ϕ into a slow parameter, and a large E_J/E_C reduces the magnitude of its quantum fluctuations. This suggests

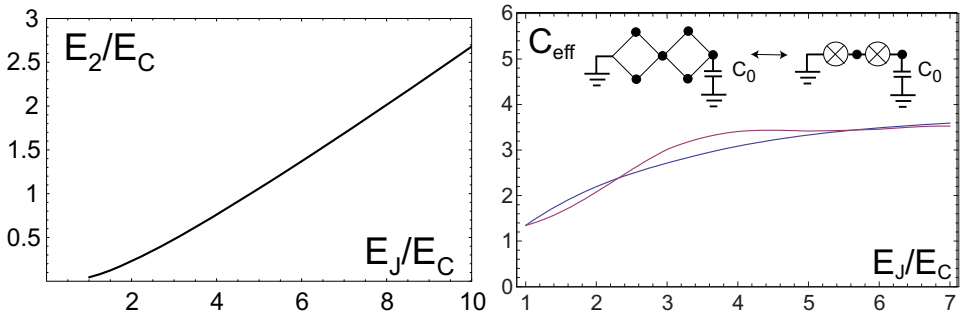

FIGURE 7. (a) The exact diagonalization result E_2 for the second harmonics of a single rhombus as a function of E_J/E_C. (b) The effective capacitance of a single rhombus as a function of E_J/E_C determined, as explained in the text, from the energy gap of a chain of two rhombi with its rightmost island connected to the ground plane by the capacitance C_0. The three curves correspond, from bottom up, to $C_0 = 2$, $C_0 = 6$, and $C_0 = 10$.

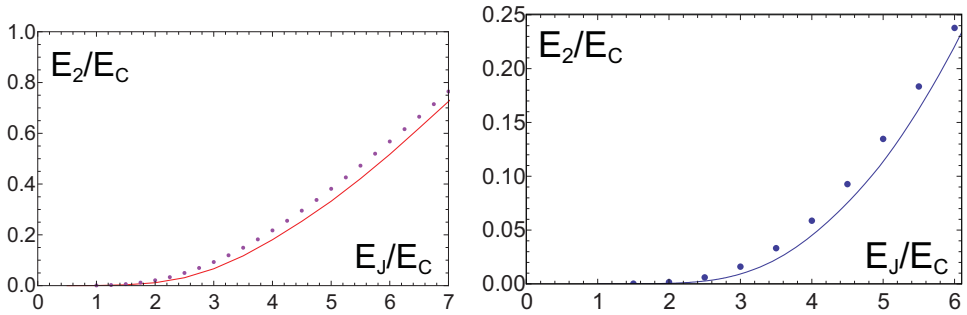

FIGURE 8. (a) The effective stiffness E_2' of a chain of two rhombi, where the phase ϕ on the rightmost island is taken as a control parameter. The plots show the results of the numerical diagonalization (dots) of the two rhombi chain, the results of the mapping onto a chain of two Z_2 junctions whose bare parameters E_2 and $E_C^{\rm eff}$ are determined as explained in the paper, and the recursive approximation for this chain of two rhombi. (b) The same curves are shown for the chain of three rhombi.

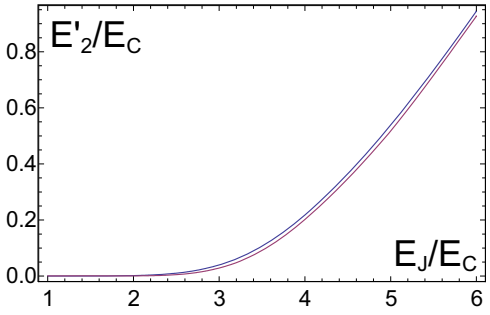

FIGURE 9. (Color online) The system of twelve rhombi at the same level of hierarchy as the system of junctions shown in Fig.6 contains 31 quantum rotors and so is too large for a direct numerical calculation. The upper (blue) line shows the result of the recursive approximation described in the text. The lower (purple) line uses the approximate mapping on the K=3 array of Z_2 junctions. The agreement between these two methods is very good.

that this way to map a network of rhombi onto the network of Z_2 junctions is likely to provide a good estimate for both the local Z_2 gap associated to the energy difference between states with even and odd particle numbers on a given node, and the phase stiffness for the charge $4e$ condensate. As a consistency check of this procedure, we compare in Fig. 8 the phase stiffness E_2' for a chain of a few rhombi, with the same quantity for a chain of Z_2 junctions. The results for $N = 2$ are shown on Fig. 8a, and those for $N = 3$ on Fig. 8b. The agreement between the rhombi chains and the appropriate Z_2 chains is very good throughout the whole range of E_J/E_C values considered here.

Another check is provided by the calculation of the stiffness for the system of twelve rhombi at the same level of hierarchy as the system of junctions shown in Fig.6, using two different approximate methods. The first one is a recursive approximation starting with the initial $4e$ tunneling amplitude of a series of two rhombi that has just been computed (see Fig. 8), and with an effective capacitance of half the effective capacitance of a single rhombus shown on Fig. 7. The second method uses the mapping onto the $K = 3$ network of Z_2 junctions represented on Fig. 6a. The results of both calculations are shown on Fig. 9, and the small difference between

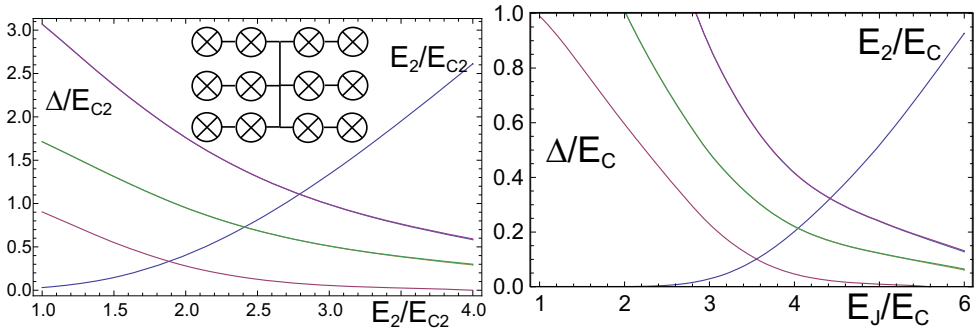

FIGURE 10. Effective phase stiffness E_2' (increasing curve) and energy gaps of low energy states (decreasing curves) of a $K = 3$ system of two rhombi chains connected to a central island, computed using the mapping onto a similar array of Z_2 junctions. These data are plotted versus the effective E_2/E_{C2} of these Z_2 junctions (a), and versus the nominal E_J of the individual junctions which compose the rhombi (b). To convert from E_2/E_{C2} to E_J/E_C we used the effective Josephson energy of the rhombus shown on Fig. 7 and the effective capacitance shown on Fig. 7. The lowest gap corresponds to one Z_2 charge on the central island, i.e. to the label $(1,0,0)$ defined in text. The second curve corresponds to two types of states, that have one Z_2 charge on one site in one of the six branches, with or without a Z_2 charge on the central island. These states, whose energies are very close, are labelled by $(0,1,0)$ and $(1,1,0)$. Finally, the upper curve is associated to the two nearly degenerate levels with labels $(0,1,1)$ and $(1,1,1)$.

the two curves is another indication that these various procedures are mutually consistent.

Low energy excitation spectrum

Here we focus on the system with twelve rhombi at the same level of the $K = 3$ hierarchy as shown on Fig. 6. We assume that the total phase difference ϕ across the system is fixed at the value 0 (or π) that minimizes the energy. In this case, and in the limit of vanishing charging energy, the phase ϕ_C of the central island can take two values modulo 2π in any classical ground-state, namely 0 and π. Once ϕ_C is known, for each subchain composed of two rhombi, we have two possible chirality configurations. Therefore, this system exhibits 2^7 classical ground-states. In the presence of finite charging energy, we expect that quantum fluctuations lift the degeneracy of these classical states, leaving instead one family of low-lying states whose energies will be computed below. Above these states, that are relatively isolated, we expect a much more dense spectrum, that results from the excitation of one or more localized Josephson plasmon mode. Our general discussion of the local Z_2 symmetry shows that a useful way to label the energy eigenstates is to keep track of the values of the local Z_2 charges on each of the seven islands. Below, we shall consider a few sectors, with at most three sites carrying a non-zero value of the Z_2 charge (that is an odd number of Cooper pairs). We shall then use labels of the form (a,b,c), with $a,b,c \in \{0,1\}$ to refer to such states, where a, b, and c indicate the Z_2 charge on the central island, on one particular site on its left, and on one particular site on its right, respectively.

Note that such an array is already too large for a numerical diagonalization of the corresponding quantum circuit Hamiltonian to be possible. Therefore, we have to rely on approximate methods, such as the mapping onto an array of Z_2 junctions, as previously discussed. Numerical results for the effective phase stiffness and the energy gaps of various excitations are presented on Fig. 10

As expected, the lowest gap is obtained while putting a single Z_2 charge on the central island, that has the smallest charging energy. This gap becomes exponentially small at large E_J/E_C, as can be expected from the semi-classical picture according to which the phase ϕ_C of the central island tunnels between its two equivalent classical minima. Note that the energy barrier between these two classical states increases when the connectivity K increases. This is in agreement with the result of Fig. 11, which shows a strong sensitivity of the gap of the $(1,0,0)$ state on the actual value of K.

By contrast, the energy of the other excited states shown here is much less sensitive to K, because these involve Z_2 charges on the chain islands. We find that the energy of two Z_2 charges on opposite sides ($(0,1,1)$ state) is a little less than twice the energy of the single Z_2 charge ($(0,1,0)$ or $(0,0,1)$). Of course, these states are degenerate, by a factor K^2 for the former and a factor $2K$ for the later. A more surprising observation is that adding an extra Z_2 charge on the central island, when one is already present elsewhere, hardly changes the energy. This can be understood in the small E_J/E_C limit by considering the inverse capacitance matrix for which the diagonal element C_{00}^{-1} on the central island is equal to twice the off-diagonal elements C_{0j}^{-1}. This implies that the states which carry the classical charges (and not

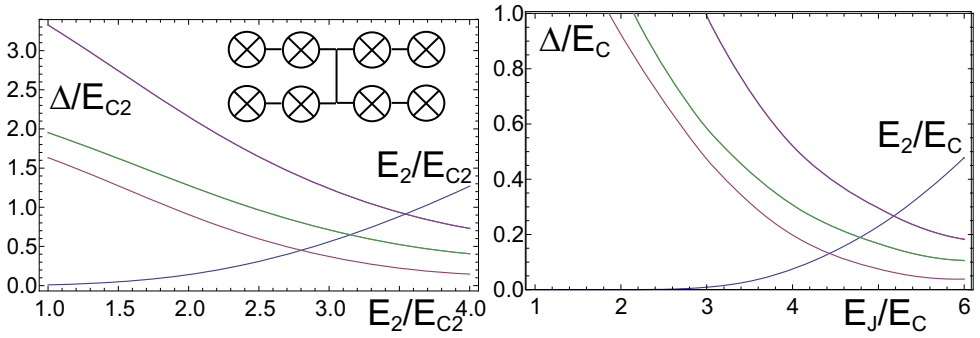

FIGURE 11. Energy gaps and effective phase stiffness for the $K = 2$ system with each chain consisting of two rhombi connected in series. The left pane gives the gaps and the stiffness for the effective Z_2 junctions, the upper pane converts these results to the physical properties of the chain made of rhombi. All notations are the same as on Fig. 10.

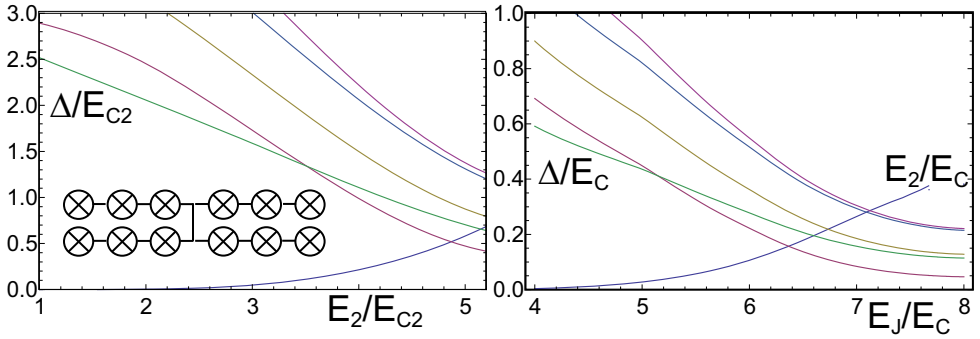

FIGURE 12. Energy gaps and effective phase stiffness for the $K = 2$ system with each chain consisting of three rhombi connected in series. The left pane gives the gaps and the stiffness for the effective Z_2 junctions, the upper pane converts these results to the physical properties of the chain made of rhombi. All notations are the same as on Fig. 10.

Z_2 charges here) $(0,1,0)$ and $(-1,1,0)$ have the same electrostatic energy, equal to $(2+1/K)E_C$. Likewise, states with charges $(0,1,-1)$ and $(-1,1,1)$ have the same electrostatic energy, $4E_C$, that is slightly less than twice the previous one. Notice that while this degeneracy is a feature of the small E_J/E_C limit, it is also expected in the semi-classical limit of large E_J/E_C, because of the exponentially small tunneling gap between to two classical states of the central island.

We have also considered another $K = 2$ system in which all the four chains connected to the central island are composed of three rhombi. The numerical results for the effective phase stiffness and for the lowest energy gaps are presented on Fig. 12. The comparison with Fig. 11 shows that this latter system has a smaller phase stiffness but larger gaps than the former $K = 2$ array with chains of only two rhombi.

As we have argued in the Introduction, for experimental implementation of a protected qubit one needs to maximize both the energy gap (to reduce the effective noise-induced tunneling amplitude of a single Cooper pair across the system) and the effective phase stiffness (to restrict the amplitude of a π shift of the phase on the central island). These conflicting requirements suggest that a good working point is obtained for the values of E_J/E_C where the curve for the effective stiffness E_2'

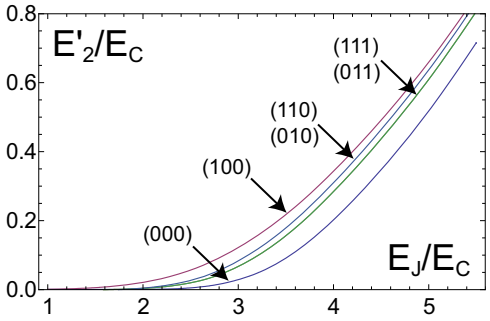

FIGURE 13. The effective phase stiffness E_2' in various excited states of the $K = 3$ array of two rhombi chains shown in Fig. 6. This quantity is directly related to the $\Phi_0/2$ periodic modulation of the critical current of the array imbedded in a large SQUID loop threaded by a magnetic flux Φ. The sensitivity of the critical current to the quantum state of the array provides a way to probe experimentally these low energy levels.

and the curve for the lowest gap cross. The optimal array is then the one that maximizes the common value of E_2' and the gap at this working point. Comparing Figs. 10, 11, and 12, we conclude that the most promising array seems to be the one with $K = 2$ composed of three rhombi chains.

PERSPECTIVES

Experimentally, the variation of the total energy for various states as a function of the total phase difference ϕ across the array can be determined by measuring the critical current of the system composed of the array in parallel with a large Josephson junction. Motivated by the theoretical analysis for rhombi chains [10, 11], the Grenoble group has shown that, in $N = 8$ rhombi chains, the critical current as a function of ϕ becomes π- periodic when the flux per rhombus is close to half a flux quantum. [12] Furthermore, they observed a clear evidence of quantum phase fluctuations in a sample with $E_J/E_C = 8$, where the critical current versus phase oscillations are rounded and reduced in amplitude. A direct experimental evidence for a finite Z_2 charge gap in the finite array corresponding to the geometry of Fig. 2 has been obtained at Rutgers, for a several samples with the ratio E_J/Ec ranging from 2 to 5.

The next important step would be to measure the energy spectrum of low lying excitations. This can still be done in principle by critical current measurements, because, as shown on Fig. 13, the global phase stiffness is sensitive to the actual quantum state of the whole array. The selective excitation of the system can be achieved by sending microwave pulses on an electrode that is capacitively coupled to the central island.

Finally, the goal is to operate such an array as a protected qubit. For the array shown on Fig. 2, the logical qubit can be encoded in the two possible values of the central island phase. A better protection would be obtained by combining two such arrays in series, using again the central island phase for encoding. As shown by Kitaev, such a system allows for a universal set of robust quantum gates. [13] We hope that the research reported here will facilitate further efforts to implement this very promising class of systems.

ACKNOWLEDGMENTS

LI is thankful to LPTMS Orsay and LPTHE Jussieu for their hospitality through a financial support from CNRS while BD has enjoyed the hospitality of the Physics Department at Rutgers University. This work was made possible by financial support from ANR grant 06BLAN-0218-01, NSF ECS-0608842 and DARPA HR0011-09-1-0009.

REFERENCES

1. A. Yu. Kitaev, arXiv:quant-ph/9707021, and Ann. Phys. (New-York) **303**, 2, (2003).
2. L. B. Ioffe, and M. V. Feigelman, Phys. Rev. B **66**, 224503, (2002).
3. B. Doucot, L. B. Ioffe and M. V. Feigelman, Phys. Rev. Lett. **90**, 107003 (2003).
4. B. Doucot, M. V. Feigelman, L. B. Ioffe and A. S. Ioselevich, Phys. Rev. B **71**, 024505 (2005).
5. D. Bacon, Phys. Rev. A **73**, 012340 (2006).
6. S. Gladchenko, D. Olaya, E. Dupont-Ferrier, B. Douçot, L. B. Ioffe, and M. E. Gershenson, Nature Phys. **5**, 48 (2009).
7. K. Park, and D. Huse, Phys. Rev. B **64**, 134522, (2001).
8. B. Douçot and J. Vidal, Phys. Rev. Lett. **88**, 227005, (2002).
9. K. A. Matveev, A. I. Larkin, and L. I. Glazman, Phys. Rev. Lett. **89**, 096802, (2002).
10. I. V. Protopopov, and M. V. Feigelman, Phys. Rev. B **70**, 184519 (2004).
11. I. V. Protopopov, and M. V. Feigelman, Phys. Rev. B **74**, 064516 (2006).
12. I. M. Pop, K. Hasselbach, O. Buisson, W. Guichard, B. Pannetier, and I. Protopopov, Phys. Rev. B **78**, 104504, (2008).
13. A. Kitaev, arXiv:cond-mat/0609441.